HHS Public Access

Author manuscript

J Magn Reson Imaging. Author manuscript; available in PMC 2020 March 17.

Published in final edited form as:

J Magn Reson Imaging. 2019 April ; 49(4): 927–938. doi:10.1002/jmri.26556.

Role of Texture Analysis in Breast MRI as a Cancer Biomarker: A Review

Rhea D. Chitalia, BS, **Despina Kontos, PhD***

Department of Radiology, University of Pennsylvania, Perelman School of Medicine & Hospital of the University of Pennsylvania, Philadelphia, Pennsylvania, USA

Abstract

Breast cancer is a known heterogeneous disease. Current clinically utilized histopathologic biomarkers may undersample tumor heterogeneity, resulting in higher rates of misdiagnosis for breast cancer. MRI can provide a whole-tumor sampling of disease burden and is widely utilized in clinical care. Texture analysis can provide a localized description of breast cancer, with particular emphasis on quantifying breast lesion heterogeneity. The object of this review is to provide an overview of texture analysis applications towards breast cancer diagnosis, prognosis, and treatment response evaluation and review the role of image-based texture features as noninvasive prognostic and predictive biomarkers.

One in eight women are diagnosed with breast cancer in the United States each year.[1,2] Breast cancer is a known heterogeneous disease, with inter- and intratumor heterogeneity demonstrated in genomic, histologic, and radiologic analyses.[3–5] Intratumor heterogeneity can manifest itself spatially, with microenvironment-specific factors driving the progression and distribution of distinct subpopulations.[6] Additionally, the dynamic behavior of breast cancer cells can lead to temporal intratumor heterogeneity, where disease presentation is altered longitudinally due to growth or in response to systemic and local therapies.[6] Currently, diagnostic, prognostic, and treatment decisions for breast cancer are made primarily on the basis of established histopathologic biomarkers originating from tissue samples acquired from core biopsy or surgical excision. While advanced treatment and management options have reduced the number of breast cancer-related deaths, 30% of women are either under- or overtreated for breast cancer.[7,8] As such, these histopathologic biomarkers may be an undersampling of the heterogeneous tumor, suggesting a clinical need for whole-tumor sampled biomarkers.

Imaging allows for noninvasive sampling of disease burden, with the ability to longitudinally monitor response to treatment.[9,10] Magnetic resonance imaging (MRI) is highly sensitive for primary lesion detection, particularly for high-risk women.[10] Specific MRI sequences such as diffusion weighted (DW) MRI and dynamic contrast-enhanced (DCE) MRI can provide further insight into tissue architecture and vascularization of and around the tumor.[11,12]

*Address reprint requests to: D.K., Rm. D702 Richards Bldg., 3700 Hamilton Walk, Philadelphia, PA 19104. despina.kontos@uphs.upenn.edu.

Current clinical analysis of MR images is largely qualitative, using DCE-MRI to identify tumor regions with contrast uptake or monitor morphologic appearance.[13]

Recent advances in medical image analysis have highlighted the implementation of computer vision principles and analytic techniques used to quantify and describe medical images.[14–16] Image texture has been previously defined as repeating patterns of local variations in gray-level intensities.[15,17] Texture analysis has most broadly been used to characterize the spatial distribution of gray-level intensities within an image, capturing image patterns usually unrecognizable or indistinguishable to the human eye. The original utilization of texture analysis can be traced back to computer vision applications for surface inspection and orientation, image and object classification, and shape determination, while current applications extend even beyond medical image analysis.[17–19] Within the scope of breast imaging, texture analysis has emerged as a quantitative, surrogate measure for breast parenchymal patterns when applied to images taken during mammographic and tomographic screenings, serving to augment conventional measures of breast percent density in breast cancer risk assessment.[20] As developments in MRI have led to improved resolution for 2D and 3D insight into the structure and function of the human body, MRI is now widely utilized for breast cancer screening, diagnosis, and treatment response.[9,21] As such, textural information extracted from MR images can have high clinical relevance.[22–30] As compared to a global or qualitative report of breast tumor appearance, texture analysis can provide a refined, local description of tumor complexity, heterogeneity, and kinetic behavior as seen in MRI. This quantitative characterization of MR images can have specific applications towards the diagnosis, prognosis, and treatment of breast cancer.

Commonly Extracted Texture Features

Texture analysis aims to extract high-throughput information characterizing image texture within a defined region of interest (ROI). For the analysis of breast lesions as presented in MRI, texture features are often extracted from an ROI selected within a segmented lesion, or from the whole lesion itself. Additionally, recent studies have shown clinical associations of texture within the peritumor region as well, emphasizing the importance of the tumor microenvironment as presented in MRI.[31,32]

The most commonly used texture features can be stratified by the statistical order of the voxel information encoded within the image. Specifically, first-order texture features include common statistical measures derived from a gray-level histogram, such as mean, median, and skewness. Second-order texture features are often derived from the co-occurrence matrix, as determined by Haralick and Shanmugam,[33] and the run-length matrix,[34] while higher-order texture features encode structural and frequency-based texture information (Fig. 1).

First Order: Gray-Level Histogram Features

A gray-level histogram can be generated by calculating a frequency count of the number of voxels of each gray-level intensity value, where the total number of discretized gray-levels is often a user-selected parameter. From the resulting histogram, first-order statistical features may be derived, including the mean, median, and variance. Higher moment features can also

be extracted from the histogram including skewness, the measure of the histogram distribution symmetry, and kurtosis, a measure of the histogram distribution shape. While many descriptors can be extracted from the histogram, they often provide cursory insight into the underlying texture, do not account for gray-level intensity spatial relationships within an image, and are dependent on user-selected parameters (Table 1).

Second Order: Gray-Level Co-Occurrence Matrix and Run-Length Features

Gray-level co-occurrence matrix (GLCM) features are the most commonly extracted texture features for MRI quantification. A GLCM encodes the frequency that two voxels of specific gray-level intensities are positioned a specified distance away from each other in a specified image orientation.[33] GLCM texture features are most often quantified in the four diagonal image orientations of 0°, 45°, 90°, and 135°. Second-order texture features can then be extracted from the co-occurrence matrix. Examples of such features include contrast, a descriptor of the intensity contrast between a pixel and its neighbor as determined by the distance parameter; correlation, a descriptor of the linear gray-level dependence; and homogeneity, a descriptor of the closeness of distribution in the co-occurrence matrix to the matrix diagonal. Other second-order features such as energy, a descriptor of the certainty of gray-level co-occurrence, and cluster shade, a descriptor of asymmetry in gray-level values, can also be extracted. Entropy, or the randomness of the GLCM, is another commonly extracted feature, often indicating image heterogeneity (Table 2). Run-length features measure the coarseness of an image in specified linear directions[34–36] (Table 3).

Higher Order: Structural and Transformation-Based

Structural texture features capture the intensity variations between central voxels and surrounding neighboring voxels[37] (Table 4). Extending texture analysis beyond the spatial orientation of gray-level intensity values, transformation-based texture features capture texture information encoded in a different space, such as the frequency space. Transformation-based methods include the Fourier transform, Gabor transform, and Wavelet transform.[38–40] The wavelet transform, in particular, is commonly used due to its ability to capture the MR images frequency content both at varying image scales and multiple specified directions.

Applications in Breast Computer-Aided Diagnosis

Computer-aided diagnosis (CAD) of breast tissue was one of the earliest applications of texture analysis in the breast.[41] Gibbs and Turnbull[42] were one of the first to apply texture analysis toward classifying breast lesions as benign or malignant. The authors reported using 2D DCE-MR images from a cohort of 79 women, of which 45 were diagnosed with breast cancer. An ROI was selected to encompass the entire lesion, within which gray-level intensity values were discretized to 32 levels. Within each lesion ROI, a co-occurrence matrix was determined for adjoining pixels in 0°, 45°, 90°, and 135° directions. The co-occurrence matrices of each direction were averaged and 14 GLCM texture features were extracted. Texture features of variance, sum entropy, and entropy were concluded to be the most significant when discriminating between benign and malignant lesions, as determined by logistic regression performance, suggesting that features quantifying image texture could

be a useful tool in lesion delineation. Subsequent studies have followed this preliminary, yet promising, conclusion by utilizing more complex measures of image texture to diagnose breast lesions as benign or malignant.[43–49] Nie et al[44] investigated the utility of breast lesion texture in parallel with lesion morphology features, using a retrospective study size of 71 women, of which 28 and 42 were diagnosed with benign and malignant lesions, respectively. Ten GLCM texture features were extracted from a co-occurrence matrix summarizing the entire lesion, while eight morphologic features were extracted as well. The study found that the performance of three texture features: GLCM entropy, GLCM Sum Average, and GLCM Homogeneity, and three morphology features resulted in an area under the curve (AUC) of the receiver operating characteristic (ROC) curve of 0.86. Holli et al[47] proposed using texture features to distinguish between cancerous and healthy breast tissue within a 15 × 15 pixel ROI, and found that, with 100% accuracy, a combined set of 277 texture features including histogram-based, GLCM, and wavelet features was able to distinguish between healthy and cancerous breast ROIs. Similar conclusions were reported by Nagarajan et al,[43] who found that GLCM-based texture features quantifying lesion heterogeneity were particularly accurate when classifying small lesions as benign or malignant. While many of these studies share similar conclusions with regard to specific texture features having high discriminatory capacities, there is a lack of literature for comparative studies performed on the same dataset with defined parameters for extracted features.

A multiparametric CAD approach was suggested by Bhooshan et al[46] leveraging T_2-weighted and T_1-weighted DCE-MRI. GLCM texture features were extracted from breast images from each imaging sequence, while kinetic features were extracted from the DCE-MR images to build a multiparametric feature vector. The study found that the multiparametric feature vector outperformed features extracted from an individual imaging sequence when differentiating between malignant and benign lesions, suggesting that texture analysis, when applied to T_2-weighted MR images, provided additional discriminatory information beyond that extracted from T_1-weighted imaging.

Traditional applications of texture analysis towards breast diagnosis largely focused on 2D texture features extracted from a 2D slice from 3D images. This idea was extended by Chen et al,[48] who extracted 3D GLCM texture features from a 3D breast lesion segmentation. The 3D GLCM features yielded a higher diagnostic accuracy than 2D GLCM features extracted from a 2D ROI, when distinguishing between malignant and benign breast lesions, showing an advantage for 3D breast lesion characterization.

Beyond CAD: Texture Analysis for Histopathologic and Molecular Subtype Classification

The promising conclusions of MRI texture analysis in breast cancer diagnosis suggest an architectural difference between the imaging presentation of benign and malignant lesions that can be quantified using texture features. Recent studies have begun extending this idea, hypothesizing that underlying tumor biological differences can be imaged using MRI and characterized using texture analysis. Consequently, many groups have employed texture analysis to distinguish between the heterogeneous histopathologic[32,45,47,50] and

molecular[51–54] subtypes of breast cancer, with a larger goal of utilizing image texture features to provide a personalized diagnosis (Table 5).

In an attempt to distinguish between invasive lobular carcinoma (ILC) and invasive ductal carcinoma (IDC), Holli et al[47] extracted a total of 277 histogram, GLCM, run-length, and wavelet features. The authors found that of these only GLCM-related features characterizing lesion complexity and randomness were significantly different between ILC and IDC lesions. Similar conclusions were reported by Waugh et al,[50] who found that entropy, a texture measure of pixel distribution randomness, was significantly different between lobular and ductal lesions, suggesting a difference in underlying growth patterns and tumor heterogeneity.

Increasing the scope of texture analysis to include the surrounding microenvironment in addition to the breast lesion, Wang et al[32] investigated the role of kinetic contrast uptake texture in differentiating between histopathologic subtypes of breast cancer. Texture features were extracted from pharmacokinetic parametric maps generated from DCE-MR images of the tumor and surrounding parenchyma. Adding texture features characterizing heterogeneous uptake in the breast parenchyma to a model containing lesion texture features allowed for the identification of triple-negative breast cancers (TNBC). The study concluded that the characterization of heterogeneity, both within the lesion as well as the surrounding parenchyma, could provide noninvasive insight into the heterogeneous tumor behavior associated with more aggressive subtypes. These results were similar to those found in previous studies,[55,56] indicating the clinical value of lesion and peritumoral contrast uptake quantification. Texture features quantifying lesion heterogeneity have also been shown to aid in delineating between molecular subtypes of breast cancer. Studies have shown a textural difference between the MR presentation of luminal A and luminal B subtypes, with luminal B lesions having a more quantifiably heterogeneous appearance.[51,54]

Texture Analysis for Breast Cancer Prognosis and Therapy Response Prediction

Recent studies have shown promising conclusions when exploring the relationship between breast lesion texture and risk of recurrence, and the value of image texture as a noninvasive prognostic biomarker[45,57–61] (Table 6). Kim et al[57] performed a retrospective analysis of 203 women diagnosed with invasive breast cancer, extracting histogram uniformity and entropy features from both T_2-weighted MR images and T_1-weighted DCE-MRI. Univariate and multivariate associations between these texture features and disease-free survival determined that increased tumor heterogeneity in T_2-weighted MRI could be used to stratify patients more at risk for recurrence. That study suggested that tumor heterogeneity, as quantified by lesion texture, could be used in MRI as an independent prognostic marker. Similar conclusions were drawn by Park et al,[59] who generated a multivariate feature vector based on morphologic, histogram texture, and GLCM texture features, from which specifically GLCM cluster tendency, GLCM variance, and GLCM sum variance were selected for in a model stratifying patients at risk for recurrence. Mahrooghy et al[60,61] extracted wavelet texture features from within tumor subregions partitioned by

pharmacokinetic behavior and concluded that the spatial frequency texture pattern captured using wavelets within the heterogeneous subregions could serve as a strong prognostic biomarker for predicting risk of tumor recurrence (AUC = 0.88).

The potential for texture analysis in breast cancer treatment has been demonstrated in recent studies, showing the potential for MRI-extracted texture features to serve as noninvasive predictive biomarkers[31,35,56,57,62–72] (Table 7). In order to predict response to treatment, some studies utilize first-order statistical texture measures extracted from the tumor ROI. Specifically, Johansen et al[71] calculated three first-order statistical features of mean, standard deviation, and prediction from a relative signal intensity histogram generated from prechemotherapy DCE-MR scans. Of these, skewness and kurtosis were found to be strongly correlated with complete response to therapy. Similarly, Padhani et al[72] conducted a retrospective study of 25 women diagnosed with primary invasive cancer, imaged using DCE-MRI before and after the first cycle of treatment. Leveraging contrast enhancement, the authors generated a histogram from a pharmacokinetic parametric map of the full lesion ROI, and concluded that responsive patients displayed a decrease in pharmacokinetic range, and proposed that this could be attributed to a decrease in heterogeneity after the first cycle of treatment.

While histogram texture can provide useful information regarding the distribution of gray-level intensity values, it is limited when capturing spatial heterogeneity within a lesion, as it largely ignores the spatial relationships between voxels. Studies extracting higher-order texture features can further quantify the relation between tumor heterogeneity and response to therapy. To this end, Teruel et al[62] extracted second-order statistical GLCM features from pharmacokinetic maps generated from DCE-MR images of women diagnosed with locally advanced breast cancer. Eight GLCM features were found to significantly differ between responders and nonresponders, and GLCM sum variance was able to predict response to treatment with an AUC of 0.77. Similar conclusions were drawn by Thibault et al,[63] who expanded this 2D analysis by extracting 3D GLCM texture features from DCE-MR pharmacokinetic parametric maps in order to predict response to neoadjuvant chemotherapy (NAC). The 3D GLCM texture features were particularly significant in identifying early responders to NAC, with results showing nonresponders having higher microvascular heterogeneity. In a retrospective study of 36 women who underwent NACT, the change in tumor heterogeneity between pretreatment and mid-treatment, as calculated by entropy and uniformity changes, was predictive of pathologic complete response (pCR) with an AUC of 0.84.[65] Comparing this performance to change in tumor size (AUC = 0.66) demonstrates a greater sensitivity for lesion texture in characterizing an early response to pCR.

Current clinical predictions for achieving pCR are based on tumor histopathologic characteristics. As intratumor heterogeneity is associated with adverse clinical outcomes, the limited tissue taken during biopsy may be inadequate for a whole-tumor-based prediction.[5,73] Michoux et al[66] performed a retrospective analysis on the DCE-MR scans of 69 patients diagnosed with IDC undergoing NAC. For each woman, texture, kinetic, and morphology-based features were extracted from within the pretreatment lesion ROI. The authors concluded that only four parameters—three texture features (GLCM inverse difference moment, gray-level nonuniformity, and long run high gray-level emphasis), and the washin

slope kinetic feature—were found to classify nonresponders with 84% sensitivity. Of particular note, clinically utilized histopathologic predictive biomarkers such as estrogen receptor (ER) status, progesterone receptor (PR) status, Ki67 status, and human epidermal growth factor receptor 2 (HER2), along with tumor grade, were not significant when classifying early response, further highlighting the utility of texture analysis. Similarly, Golden et al[64] extracted GLCM-based texture features from pharmacokinetic parametric maps generated from DCE-MR images of women diagnosed with TNBC, in order to predict pCR, residual lymph node metastases, and residual tumor with lymph node metastases. The predictive performance of GLCM texture features was compared to "patterns of response," a qualitative description of lesion appearance before and after chemotherapy, as determined by a radiologist. The GLCM texture features extracted from prechemotherapy MR images could predict pCR and residual lymph node metastasis with a reported AUC of 0.68 when classified in a logistic regression model. In contrast, the radiologist determined "patterns of response" did not predict any of three outcome measures.

The conclusions drawn from studies implementing texture analysis for breast cancer diagnosis, prognosis, and treatment suggest that texture features demonstrating increased lesion heterogeneity are associated with aggressive growth, unfavorable prognosis, and poor treatment outcomes.[31,57,61,67,74–76] In addition, they propose a method for noninvasively quantifying the underlying biology of tumor subregions driving recurrence, response, and resistance to therapy (Fig. 2).

Texture Analysis Study Designs

Effective use of texture analysis on MR images of breast cancer is highly dependent on appropriate study design and statistical evaluation. There are numerous methods for texture feature extraction, resulting in a myriad of ways to quantify an image's texture. Consequently, having a high-dimensional texture feature set as compared to a relatively smaller sample size can result in the overfitting of a statistical learning model, resulting in false-positive classification and over-or underestimated statistical associations. Additionally, redundant texture features can often decrease performance accuracy. To alleviate this, methods such as principal component analysis or independent component analysis can be used to reduce the dimensionality of the texture feature set.[77] Feature selection methods can also be used to reduce texture feature redundancy and promote relevant texture features for analysis. Statistical correction methods, such as the Benjamini–Hochberg correction,[78] can be used to reduce false positives in statistical association conclusions. Ideally, results should be validated using an independent dataset, to ensure the veracity of the texture analysis. While finding comparable independent datasets is not always feasible, splitting the initial dataset into discovery and validation sets is an alternative solution to ensure repeatability. Similarly, crossvalidation can be used to identify robust conclusions. Lastly, utilization of publicly available datasets and detailed methodology of specific texture parameters used during feature extraction can allow for study repeatability.

Future Directions

Texture analysis is limited by user-defined feature parameters, such as selecting the number of discretized gray levels within an image, MR acquisition protocol, and image quality.[15,48,79] As such, the literature largely lacks repeated studies performed on the same datasets with standardized texture feature extraction. Additionally, while texture features provide quantitative measures of breast tumor texture, the direct biological interpretation of specific texture feature values remains largely uncertain. Leveraging the specific properties of various functional MRI imaging techniques, texture analysis can be used to quantify different tissue properties. Texture analysis applied to DCE-MRI or DW-MRI could provide insight on the distribution or longitudinal development of tumor vascularization and diffusion, respectively. Similarly, statistical associations between image-derived texture features and histopathologic or genomic expression data could lead to a biological basis for tumor texture. Further work is needed to explore the relationships between specific texture features and underlying biology.

Many studies aiming to analyze MRI presentations of breast lesions for diagnostic, prognostic, and treatment applications have expanded the number and type of features extracted to include morphology, texture, and pharmacokinetic features, allowing for a thorough and quantitative characterization of all tumor properties. This has developed into the new field of “radiomics,” broadly defined as the extraction of high-throughput quantitative features from images obtained from medical imaging modalities.[80–82] The promising conclusions from studies employing texture analyses have demonstrated that features defining high lesion heterogeneity have been associated with more aggressive diagnoses and poor response to treatment. Benefited by the whole-tumor sampling and visualization of tumor vasculature afforded by MRI, one of the largest aims in radiomics is to accurately characterize and quantify intratumor heterogeneity.[4,5,73] Current advances within radiomics also include quantifying underlying tumor biology by investigating relationships between radiomic features extracted from complementary imaging modalities,[83] gene expression pathways,[53,84] and existing clinical definitions for breast cancer.[85,86] Additionally, leveraging radiomic information from alternative imaging modalities in combination with that acquired from MRI could augment breast tumor characterization.[87] Moving forward, radiomic analysis has the potential for use in fully characterizing tumor biology to serve as a noninvasive, quantitative tumor assay, complementing proteomic and genomic tumor analyses for a comprehensive and personalized understanding of breast cancer.

References

1. Tao Z, Shi A, Lu C, Song T, Zhang Z, Zhao J. Breast cancer: Epidemiology and etiology. Cell Biochem Biophys 2015;72:333–338. [PubMed: 25543329]
2. DeSantis C, Ma J, Bryan L, Jemal A. Breast cancer statistics, 2013. CA Cancer J Clin 2014;64:52–62. [PubMed: 24114568]
3. Marusyk A, Polyak K. Tumor heterogeneity: Causes and consequences. Biochim Biophys Acta Rev Cancer 2010;1805:105–117.
4. Polyak K. Heterogeneity in breast cancer. J Clin Invest 2011;121: 3786–3788. [PubMed: 21965334]

5. O'Connor JP, Rose CJ, Waterton JC, Carano RA, Parker GJ, Jackson A. Imaging intratumor heterogeneity: Role in therapy response, resistance, and clinical outcome. Clin Cancer Res 2015;21:249–257. [PubMed: 25421725]
6. Dagogo-Jack I, Shaw AT. Tumour heterogeneity and resistance to cancer therapies. Nat Rev Clin Oncol 2018;15:81–94. [PubMed: 29115304]
7. Bedard PL, Cardoso F. Can some patients avoid adjuvant chemotherapy for early-stage breast cancer? Nat Rev Clin Oncol 2011;8:272. [PubMed: 21364525]
8. Sabatier R, Gonçalves A, Bertucci F. Personalized medicine: Present and future of breast cancer management. Crit Rev Oncol Hematol 2014;91: 223–233. [PubMed: 24725667]
9. Gavenonis SC, Roth SO. Role of magnetic resonance imaging in evaluating the extent of disease. Magn Reson Imaging Clin 2010;18:199–206.
10. Weinstein S, Rosen M. Breast MR imaging: Current indications and advanced imaging techniques. Radiol Clin 2010;48:1013–1042.
11. Tse GM, Chaiwun B, Wong KT, et al. Magnetic resonance imaging of breast lesions—A pathologic correlation. Breast Cancer Res Treat 2007; 103:1–10. [PubMed: 17033923]
12. Hylton NM. Vascularity assessment of breast lesions with gadolinium-enhanced MR imaging. Magn Reson Imaging Clin N Am 2001;9: 321–332, vi. [PubMed: 11493422]
13. O'Connor JP, Jackson A, Asselin M-C, Buckley DL, Parker GJ, Jayson GC. Quantitative imaging biomarkers in the clinical development of targeted therapeutics: Current and future perspectives. Lancet Oncol 2008;9:766–776. [PubMed: 18672212]
14. McInerney T, Terzopoulos D. Deformable models in medical image analysis: A survey. Med Image Anal 1996;1:91–108. [PubMed: 9873923]
15. Castellano G, Bonilha L, Li L, Cendes F. Texture analysis of medical images. Clin Radiol 2004;59:1061–1069. [PubMed: 15556588]
16. Ganeshan B, Miles KA. Quantifying tumour heterogeneity with CT. Cancer Imaging 2013;13:140. [PubMed: 23545171]
17. Jain R, Kasturi R, Schunck BG. Machine vision. New York: McGraw-Hill; 1995.
18. Jain A, Ross A, Prabhakar S. Fingerprint matching using minutiae and texture features In: 2001 Proceedings 2001 International Conference on Image Processing, Vol. 3: IEEE; 2001 p 282–285.
19. Chen K, Wei H, Hennebert J, Ingold R, Liwicki M. Page segmentation for historical handwritten document images using color and texture features Frontiers in Handwriting Recognition (ICFHR), 2014 14th International Conference on: IEEE; 2014 p 488–493.
20. Gastounioti A, Conant EF, Kontos D. Beyond breast density: A review on the advancing role of parenchymal texture analysis in breast cancer risk assessment. Breast Cancer Res 2016;18:91. [PubMed: 27645219]
21. Morrow M, Waters J, Morris E. MRI for breast cancer screening, diagnosis, and treatment. Lancet 2011;378:1804–1811. [PubMed: 22098853]
22. Holli KK, Harrison L, Dastidar P, et al. Texture analysis of MR images of patients with mild traumatic brain injury. BMC Med Imaging 2010;10:8. [PubMed: 20462439]
23. Hackmack K, Paul F, Weygandt M, Allefeld C, Haynes J-D, Initiative AsDN. Multi-scale classification of disease using structural MRI and wavelet transform. Neuroimage 2012;62:48–58. [PubMed: 22609452]
24. Mayerhoefer ME, Breitenseher MJ, Kramer J, Aigner N, Hofmann S, Materka A. Texture analysis for tissue discrimination on T1-weighted MR images of the knee joint in a multicenter study: Transferability of texture features and comparison of feature selection methods and classifiers. J Magn Reson Imaging 2005;22:674–680. [PubMed: 16215966]
25. Michopoulou S, Costaridou L, Vlychou M, Speller R, Todd-Pokropek A. Texture-based quantification of lumbar intervertebral disc degeneration from conventional T2-weighted MRI. Acta Radiol 2011;52:91–98. [PubMed: 21498333]
26. Vignati A, Mazzetti S, Giannini V, et al. Texture features on T2-weighted magnetic resonance imaging: New potential biomarkers for prostate cancer aggressiveness. Phys Med Biol 2015;60:2685. [PubMed: 25768265]

27. Assefa D, Keller H, Ménard C, Laperriere N, Ferrari RJ, Yeung I. Robust texture features for response monitoring of glioblastoma multiforme on-weighted and-FLAIR MR images: A preliminary investigation in terms of identification and segmentation. Med Phys 2010;37:1722–1736. [PubMed: 20443493]
28. Torheim T, Malinen E, Kvaal K, et al. Classification of dynamic contrast enhanced MR images of cervical cancers using texture analysis and support vector machines. IEEE Trans Med Imaging 2014;33:1648–1656. [PubMed: 24802069]
29. Harrison L, Dastidar P, Eskola H, et al. Texture analysis on MRI images of non-Hodgkin lymphoma. Comput Biol Med 2008;38:519–524. [PubMed: 18342845]
30. Zhang Y. MRI texture analysis in multiple sclerosis. J Biomed Imaging 2012;2012:2.
31. Braman NM, Etesami M, Prasanna P, et al. Intratumoral and peritumoral radiomics for the pretreatment prediction of pathological complete response to neoadjuvant chemotherapy based on breast DCE-MRI. Breast Cancer Res 2017;19:57. [PubMed: 28521821]
32. Wang J, Kato F, Oyama-Manabe N, et al. Identifying triple-negative breast cancer using background parenchymal enhancement heterogeneity on dynamic contrast-enhanced MRI: A pilot radiomics study. PLoS One 2015;10:e0143308. [PubMed: 26600392]
33. Haralick RM, Shanmugam K. Textural features for image classification. IEEE Trans Syst Man Cybernet 1973:610–621.
34. Galloway MM. Texture analysis using grey level run lengths. NASA STI/-Recon Technical Report N 1974;75.
35. Tang X. Texture information in run-length matrices. IEEE Trans Image Process 1998;7:1602–1609. [PubMed: 18276225]
36. Chu A, Sehgal CM, Greenleaf JF. Use of gray value distribution of run lengths for texture analysis. Pattern Recogn Lett 1990;11:415–419.
37. Ojala T, Pietikainen M, Maenpaa T. Multiresolution gray-scale and rotation invariant texture classification with local binary patterns. IEEE Trans Pattern Anal Mach Intell 2002;24:971–987.
38. Porter R, Canagarajah N. Robust rotation-invariant texture classification: Wavelet, Gabor filter and GMRF based schemes. IEEE Proc Vis Image Sign Process 1997;144:180–188.
39. Srinivasan G, Shobha G. Statistical texture analysis. In: Proc World Acad Sci Eng Technol Vol. 36; 2008 p 1264–1269.
40. Livens S, Scheunders P, Van de Wouwer G, Van Dyck D. Wavelets for texture analysis, an overview. 1997.
41. Cho GY, Moy L, Kim SG, et al. Evaluation of breast cancer using intra-voxel incoherent motion (IVIM) histogram analysis: Comparison with malignant status, histological subtype, and molecular prognostic factors. Eur Radiol 2016;26:2547–2558. [PubMed: 26615557]
42. Gibbs P, Turnbull LW. Textural analysis of contrast-enhanced MR images of the breast. Magn Reson Med 2003;50:92–98. [PubMed: 12815683]
43. Nagarajan MB, Huber MB, Schlossbauer T, Leinsinger G, Krol A, Wismüller A. Classification of small lesions in breast MRI: Evaluating the role of dynamically extracted texture features through feature selection. J Med Biol Eng 2013;33(1).
44. Nie K, Chen J-H, Hon JY, Chu Y, Nalcioglu O, Su M-Y. Quantitative analysis of lesion morphology and texture features for diagnostic prediction in breast MRI. Acad Radiol 2008;15:1513–1525. [PubMed: 19000868]
45. Bhooshan N, Giger ML, Jansen SA, Li H, Lan L, Newstead GM. Cancerous breast lesions on dynamic contrast-enhanced MR images: Computerized characterization for image-based prognostic markers. Radiology 2010;254:680–690. [PubMed: 20123903]
46. Bhooshan N, Giger M, Lan L, et al. Combined use of T2-weighted MRI and T1-weighted dynamic contrast-enhanced MRI in the automated analysis of breast lesions. Magn Reson Med 2011;66:555–564. [PubMed: 21523818]
47. Holli K, Lääperi A-L, Harrison L, et al. Characterization of breast cancer types by texture analysis of magnetic resonance images. Acad Radiol 2010;17:135–141. [PubMed: 19945302]
48. Chen W, Giger ML, Li H, Bick U, Newstead GM. Volumetric texture analysis of breast lesions on contrast-enhanced magnetic resonance images. Magn Reson Med 2007;58:562–571. [PubMed: 17763361]

49. Issa B, Buckley DL, Turnbull LW. Heterogeneity analysis of Gd-DTPA uptake: Improvement in breast lesion differentiation. J Comput Assist Tomogr 1999;23:615–621. [PubMed: 10433296]
50. Waugh S, Purdie C, Jordan L, et al. Magnetic resonance imaging texture analysis classification of primary breast cancer. Eur Radiol 2016;26: 322–330. [PubMed: 26065395]
51. Holli-Helenius K, Salminen A, Rinta-Kiikka I, et al. MRI texture analysis in differentiating luminal A and luminal B breast cancer molecular subtypes-a feasibility study. BMC Med Imaging 2017;17:69. [PubMed: 29284425]
52. Sutton EJ, Oh JH, Dashevsky BZ, et al. Breast cancer subtype intertumor heterogeneity: MRI-based features predict results of a genomic assay. J Magn Reson Imaging 2015;42:1398–1406. [PubMed: 25850931]
53. Li H, Zhu Y, Burnside ES, et al. MR imaging radiomics signatures for predicting the risk of breast cancer recurrence as given by research versions of MammaPrint, Oncotype DX, and PAM50 gene assays. Radiology 2016;281:382–391. [PubMed: 27144536]
54. Wu J, Sun X, Wang J, et al. Identifying relations between imaging phenotypes and molecular subtypes of breast cancer: Model discovery and external validation. J Magn Reson Imaging 2017;46:1017–1027. [PubMed: 28177554]
55. King V, Brooks JD, Bernstein JL, Reiner AS, Pike MC, Morris EA. Back-ground parenchymal enhancement at breast MR imaging and breast cancer risk. Radiology 2011;260:50–60. [PubMed: 21493794]
56. Chamming's F, Ueno Y, Ferré R, et al. Features from computerized texture analysis of breast cancers at pretreatment MR imaging are associated with response to neoadjuvant chemotherapy. Radiology 2017;286: 412–420. [PubMed: 28980886]
57. Kim J-H, Ko ES, Lim Y, et al. Breast cancer heterogeneity: MR imaging texture analysis and survival outcomes. Radiology 2016;282:665–675. [PubMed: 27700229]
58. Pickles MD, Lowry M, Gibbs P. Pretreatment prognostic value of dynamic contrast-enhanced magnetic resonance imaging vascular, texture, shape, and size parameters compared with traditional survival indicators obtained from locally advanced breast cancer patients. Invest Radiol 2016;51:177–185. [PubMed: 26561049]
59. Park H, Lim Y, Ko ES, et al. Radiomics signature on magnetic resonance imaging: Association with disease-free survival in patients with invasive breast cancer. Clin Cancer Res 2018;37832017.
60. Mahrooghy M, Ashraf AB, Daye D, et al. Heterogeneity wavelet kinetics from DCE-MRI for classifying gene expression based breast cancer recurrence risk In: International Conference on Medical Image Computing and Computer-Assisted Intervention. Berlin: Springer; 2013 p 295–302.
61. Mahrooghy M, Ashraf AB, Daye D, et al. Pharmacokinetic tumor heterogeneity as a prognostic biomarker for classifying breast cancer recurrence risk. IEEE Trans Biomed Eng 2015;62:1585–1594. [PubMed: 25622311]
62. Teruel J, Heldahl M, Goa P, et al. Dynamic contrast-enhanced MRI texture analysis for pretreatment prediction of clinical and pathological response to neoadjuvant chemotherapy in patients with locally advanced breast cancer. NMR Biomed 2014;27:887–896. [PubMed: 24840393]
63. Thibault G, Tudorica A, Afzal A, et al. DCE-MRI texture features for early prediction of breast cancer therapy response. Tomography 2017;3:23. [PubMed: 28691102]
64. Golden DI, Lipson JA, Telli ML, Ford JM, Rubin DL. Dynamic contrast-enhanced MRI-based biomarkers of therapeutic response in triple-negative breast cancer. J Am Med Inform Assoc 2013;20:1059–1066. [PubMed: 23785100]
65. Parikh J, Selmi M, Charles-Edwards G, et al. Changes in primary breast cancer heterogeneity may augment midtreatment MR imaging assessment of response to neoadjuvant chemotherapy. Radiology 2014;272: 100–112. [PubMed: 24654970]
66. Michoux N, Van den Broeck S, Lacoste L, et al. Texture analysis on MR images helps predicting non-response to NAC in breast cancer. BMC Cancer 2015;15:574. [PubMed: 26243303]
67. Wu J, Gong G, Cui Y, Li R. Intratumor partitioning and texture analysis of dynamic contrast-enhanced (DCE)-MRI identifies relevant tumor subregions to predict pathological response of

breast cancer to neoadjuvant chemotherapy. J Magn Reson Imaging 2016;44:1107–1115. [PubMed: 27080586]

68. Ashraf A, Gaonkar B, Mies C, et al. Breast DCE-MRI kinetic heterogeneity tumor markers: Preliminary associations with neoadjuvant chemotherapy response. Transl Oncol 2015;8:154–162. [PubMed: 26055172]
69. Ahmed A, Gibbs P, Pickles M, Turnbull L. Texture analysis in assessment and prediction of chemotherapy response in breast cancer. J Magn Reson Imaging 2013;38:89–101. [PubMed: 23238914]
70. El Adoui M, Drisis S, Larhmam M, Lemort M, Benjelloun M. Breast cancer heterogeneity analysis as index of response to treatment using MRI images: A review. Imaging Med 2017;9:109–119.
71. Johansen R, Jensen LR, Rydland J, et al. Predicting survival and early clinical response to primary chemotherapy for patients with locally advanced breast cancer using DCE-MRI. J Magn Reson Imaging 2009; 29:1300–1307. [PubMed: 19472387]
72. Padhani AR, Hayes C, Assersohn L, et al. Prediction of clinicopathologic response of breast cancer to primary chemotherapy at contrast-enhanced MR imaging: Initial clinical results. Radiology 2006;239:361–374. [PubMed: 16543585]
73. Sala E, Mema E, Himoto Y, et al. Unravelling tumour heterogeneity using next-generation imaging: Radiomics, radiogenomics, and habitat imaging. Clin Radiol 2017;72:3–10. [PubMed: 27742105]
74. Burnside ES, Drukker K, Li H, et al. Using computer-extracted image phenotypes from tumors on breast magnetic resonance imaging to predict breast cancer pathologic stage. Cancer 2016;122:748–757. [PubMed: 26619259]
75. Agner SC, Rosen MA, Englander S, et al. Computerized image analysis for identifying triple-negative breast cancers and differentiating them from other molecular subtypes of breast cancer on dynamic contrast-enhanced MR images: A feasibility study. Radiology 2014;272:91–99. [PubMed: 24620909]
76. Zhu Y, Li H, Guo W, et al. Deciphering genomic underpinnings of quantitative MRI-based radiomic phenotypes of invasive breast carcinoma. Sci Rep 2015;5:17787. [PubMed: 26639025]
77. Duda R, Hart PE, Stork DG. Pattern classification and scene analysis. New York: John Wiley & Sons; 2000.
78. Benjamini Y, Hochberg Y. Controlling the false discovery rate: A practical and powerful approach to multiple testing. J R Stat Soc B 1995:289–300.
79. Waugh SA, Lerski RA, Bidaut L, Thompson AM. The influence of field strength and different clinical breast MRI protocols on the outcome of texture analysis using foam phantoms. Med Phys 2011;38:5058–5066. [PubMed: 21978050]
80. Lambin P, Rios-Velazquez E, Leijenaar R, et al. Radiomics: Extracting more information from medical images using advanced feature analysis. Eur J Cancer 2012;48:441–446. [PubMed: 22257792]
81. Gillies RJ, Kinahan PE, Hricak H. Radiomics: Images are more than pictures, they are data. Radiology 2015;278:563–577. [PubMed: 26579733]
82. Kumar V, Gu Y, Basu S, et al. Radiomics: The process and the challenges. Magn Reson Imaging 2012;30:1234–1248. [PubMed: 22898692]
83. Vallières M, Freeman CR, Skamene SR, El Naqa I. A radiomics model from joint FDG-PET and MRI texture features for the prediction of lung metastases in soft-tissue sarcomas of the extremities. Phys Med Biol 2015;60:5471. [PubMed: 26119045]
84. Guo W, Li H, Zhu Y, et al. Prediction of clinical phenotypes in invasive breast carcinomas from the integration of radiomics and genomics data. J Med Imaging 2015;2:041007.
85. Koo HR, Cho N, Song IC, et al. Correlation of perfusion parameters on dynamic contrast-enhanced MRI with prognostic factors and subtypes of breast cancers. J Magn Reson Imaging 2012;36:145–151. [PubMed: 22392859]
86. Li H, Zhu Y, Burnside ES, et al. Quantitative MRI radiomics in the prediction of molecular classifications of breast cancer subtypes in the TCGA/T-CIA data set. NPJ Breast Cancer 2016;2:16012. [PubMed: 27853751]

87. Lubner MG, Smith AD, Sandrasegaran K, Sahani DV, Pickhardt PJ. CT texture analysis: Definitions, applications, biologic correlates, and challenges. RadioGraphics 2017;37:1483–1503. [PubMed: 28898189]

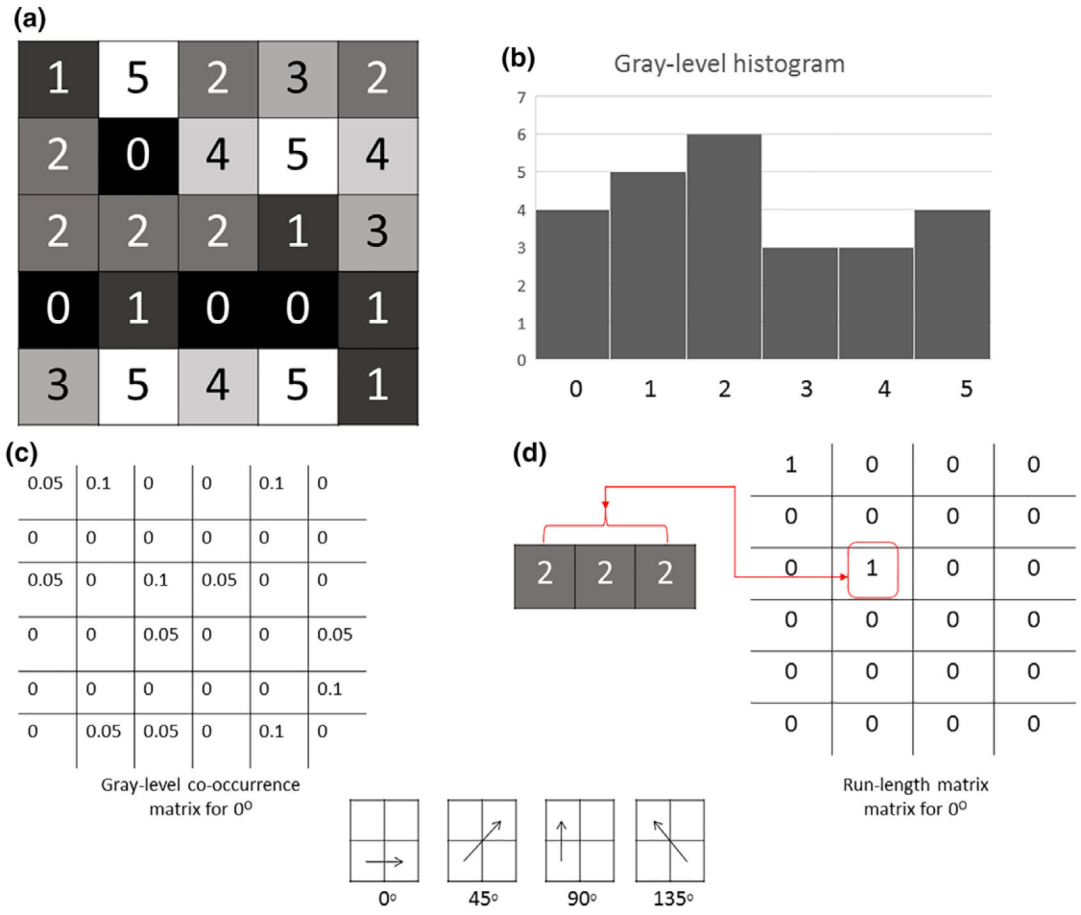

FIGURE 1:

Representative 5 × 5 pixel image with six possible gray levels (0–5) (a). Gray-level histogram generated from representative image (b). Gray-level co-occurrence matrix generated for 0°. The co-occurrence matrix encodes the frequency that two pixels are located a specific distance (1 pixel) away from one another (c). Run-length matrix generated for 0°. Run-length matrix encodes the coarseness of an image in a specified linear direction (d).

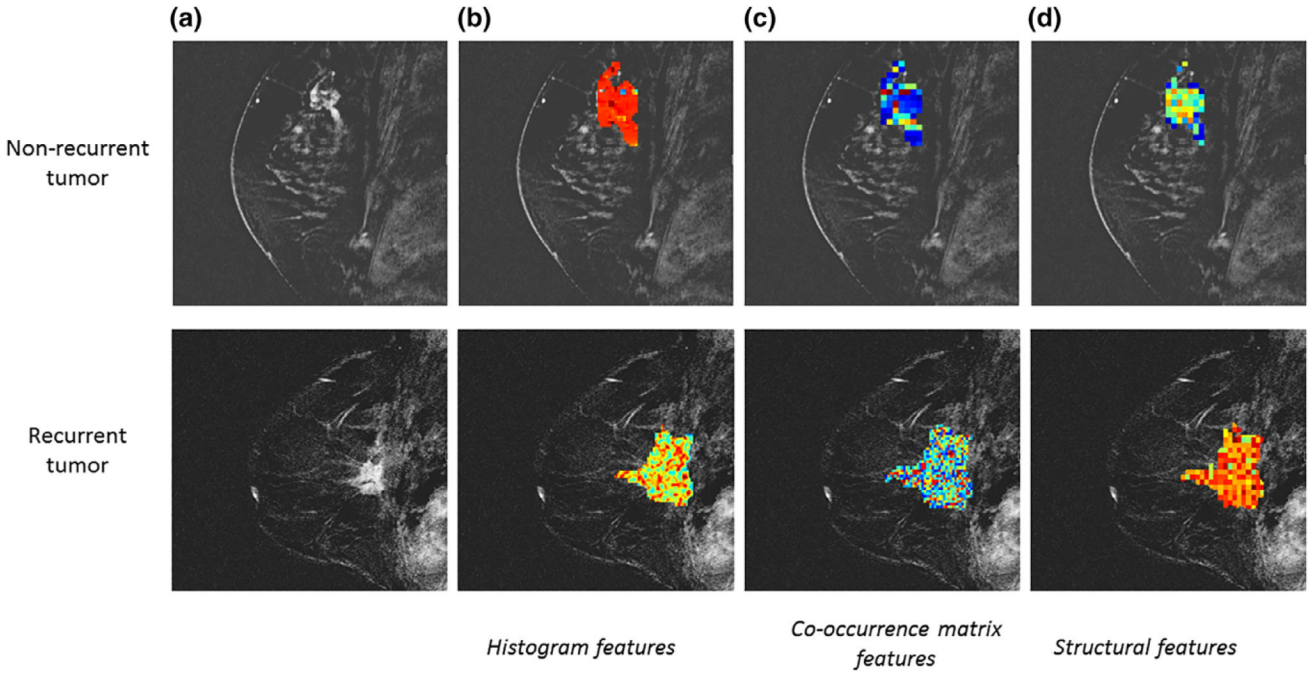

FIGURE 2:

Representative images of a nonrecurrent and recurrent breast tumor (a). Examples of texture feature maps showing distributions of histogram texture features (b), co-occurrence matrix texture features (c), and structural texture features (d).

TABLE 1.

Gray-Level Histogram Texture Features

Gray-level histogram features	Qualitative description	Mathematical description
Mean	Mean gray-level value	$\sum k \frac{k * g(k)}{\sum kg(k)}$
Min	Min gray-level value	Min(k)
Max	Max gray-level value	Max(k)
5th Percentile	Histogram bin that 5% of gray-level values are less than or equal to	k: 5% of values ≤ k
Mean 5th	Mean value of gray-level values that 5% of gray-level values are less than or equal to	$\frac{\sum_k k * g(k)}{\sum kg(k)}$ for $k \leq$ fifth percentile
95th Percentile	Histogram bin that 95% of gray-level values are greater than or equal to	k: 95% of values ≥ k
Mean 95th	Mean value of gray-level values that 95% of gray-level values are greater than or equal to	$\frac{\sum_k k * g(k)}{\sum kg(k)}$ for $k \geq$ ninety-fifth percentile
Sum	Sum of gray-level values	$\sum_k k * g(k)$
Sigma	Measure of variation of gray-level values around the mean	$\sqrt{\sum_k (k-\mu)^2 * g(k)}$
Entropy	Measure of histogram nonuniformity	$-\sum_k g(k) * \log(g(k))$
Kurtosis	Measure of histogram flatness	$\sigma^{-4} \sum_k (k-\mu)^4 * g(k) - 3$
Skewness	Measure of histogram symmetry	$\sigma^{-3} \sum_k (k-\mu)^3 * g(k)$

TABLE 2.

Representative Gray-Level Co-Occurrence Matrix Texture Features

Co-occurrence matrix features	Qualitative	description
Contrast	Intensity contrast between pixel and its neighbor	$\sum_{ij} \lvert i-j \rvert^2 f(i,j)$
Correlation	Linear gray-level dependence	$\sum_{ij} \frac{\left((i-\mu_i) * \left(j-\mu_j\right) * f(i,j)\right)}{\sigma_i \sigma_j}$
Homogeneity	Closeness of distribution in co-occurrence matrix to matrix diagonal	$\sum_{ij} \frac{f(i,j)}{1+\lvert i-j \rvert}$
Energy	Certainty of gray-level co-occurrence	$\sum_{ij} f(i,j)^2$
Entropy	Uncertainty of gray-level co-occurrence	$-\sum_{ij} f(i,j) * \log(f(i,j))$
Inverse difference moment (IDM)	Local homogeneity in gray-level co-occurrence	$\sum_{ij} \frac{f(i,j)}{\left(1+(i-j)^2\right)}$
Cluster shade	Asymmetry in gray-level values	$\sum_{ij} \left(i-\mu_i+j-\mu_j\right)^3 * f(i,j)$

TABLE 3.

Run-Length Texture Features

Run-length features		
Short run emphasis (SRE)	Emphasis on short runs	$1/n_r \sum_{i=1}^{M} \sum_{j=1}^{N} \frac{(R(i,j))}{j^2}$
Long run emphasis (LRE)	Emphasis on long runs	$1/n_r \sum_{i=1}^{M} \sum_{j=1}^{N} (R(i,j)) * j^2$
Gray-level nonuniformity (GLN)	Degree of gray-level run dissimilarity	$1/n_r \sum_{i=1}^{M} \left(\sum_{j=1}^{N} (R(i,j)) \right)^2$
Run length nonuniformity (RLN)	Dissimilarity in length of runs	$1/n_r \sum_{j=1}^{N} \left(\sum_{i=1}^{M} R(i,j) \right)^2$
Run percentage (RP)	Distribution of runs	$\frac{n_r}{\#pixels}$
Low gray-level run emphasis (LGRE)	Emphasis on low gray-level values	$1/n_r \sum_{i=1}^{M} \sum_{j=1}^{N} \frac{(R(i,j))}{(i+j)^2}$
High gray-level run emphasis (HGRE)	Emphasis on high gray-level values	$1/n_r \sum_{i=1}^{M} \sum_{j=1}^{N} (R(i,j)) * i^2$
Short run low gray-level emphasis (SRLGE)	Emphasis on short runs with low gray-level values	
Short run high gray-level emphasis (SRHGE)	Emphasis on short runs with high gray-level values	$1/n_r \sum_{i=1}^{M} \sum_{j=1}^{N} \frac{(R(i,j))(i+j)^2}{j^2}$

nr is the total number of runs, R(*i,j*) represents the number of runs with pixels of gray-level intensity value, *i*, and length of run, *j*. In all, 128 gray levels were used. Estimated by averaging over 0 °, 45°, 90°, and 135 ° orientations.

TABLE 4.

Structural Texture Features

Structural feature	Qualitative description	Mathematical description
Local Binary Pattern (LBP)	Intensity variation between a pixel and its neighboring pixels.	$LBP(x_c, y_c) = \sum_{p=0}^{P-1} q(I_p - I_c)2^P, (x_p, y_p) = \left[x_c + Qcos\left(\frac{2\pi p}{P}\right), y_c - Qsin\left(\frac{2\pi p}{P}\right)\right]$ I_c and I_p are gray-level intensity values for pixel (x_c,y_c) and pixel (x_p,y_p). q = indicator function, 0 for negative inputs and 1 for non-negative inputs.Q, P = parameters to set pixel neighborhood size, set to 1 and 8, respectively.[39,40]

TABLE 5.

Texture Analysis Studies for Breast Cancer Histopathologic and Molecular Subtype Classification

Study	Study size	Acquisition	Texture features	Findings
Holli-Helenius et al[51]	27	T1-weighted, nonfat-saturated DCE-MRI	GLCM texture features	Sum entropy and sum variance differentiate between luminal A and luminal B subtypes (AUC = 0.88)
Waugh et al[50]	200	DCE-MRI	GLCM texture features	Entropy significantly different between ILC and IDC cancers
Sutton et al[52]	178	T1-weighted fat suppressed MRI	Gray-level histogram, GLCM texture features	Features quantifying heterogeneity were able to classify between molecular subtypes
Wang et al[32]	84	DCE-MRI	Gray-level histogram, GLCM texture features	Adding texture features quantifying tumor microenvironment heterogeneity to model with features quantifying lesion heterogeneity improved classification performance to identify TNBC.
Chen et al[48]	121	T1-weighted DCE-MRI	GLCM texture features	3D texture features showed better performance than 2D texture features when classifying breast lesions as benign or malignant

J Magn Reson Imaging. Author manuscript; available in PMC 2020 March 17.

TABLE 6.

Texture Analysis Studies for Breast Cancer Prognosis

Study	Study size	Acquisition	Texture features	Findings
Kim et al[57]	203	T2-weighted and T1-weighted DCE-MRI	Histogram uniformity, histogram entropy	Heterogeneous lesions on T2-weighted imaging predicted poor RFS
Park et al[59]	294	DCE-MRI	GLCM texture features	Features characterizing high heterogeneity showed relationship to poor survival outcomes
Mahrooghy et al[61]	56	DCE-MRI	Wavelet features extracted from lesions partitioned by pharmacokinetic uptake patterns	Heterogeneity wavelet features classified tumors by risk of recurrence with AUC = 0.88

TABLE 7.

Texture Analysis Studies for Breast Cancer Treatment Response Prediction

Study	Study size	Acquisition	Texture features	Findings
Teruel et al[62]	58	T1-weighted DCE-MRI	GLCM texture features	Entropy and sum variance were most significant in predicting stable disease vs. complete responders (AUC = 0.77) and predicting pCR (AUC = 0.69), respectively
Thibault et al[63]	38	DCE-MRI	GLCM, run length features extracted from pharmacokinetic maps	GLCM features most predictive of therapy response
Golden et al[64]	60	DCE-MRI	GLCM texture features extracted from pharmacokinetic maps	Pretherapy features can predict pCR and residual lymph node metastasis
Parikh et al[65]	36	T2-and T1-weighted DCE-MRI	Entropy and uniformity	Responders to NACT showed increase in lesion homogeneity after one round of therapy
Michoux et al[66]	69	T1-weighted DCE-MRI	GLCM, run-length	Model with three texture features and one kinetic feature identified nonresponders to NAC with 84% sensitivity
Braman et al[31]	117	T1-weighted DCE-MRI	Gabor, GLCM, Laws energy measures	Intratumor and peritumor texture features predicted pCR with AUC = 0.78